


RESEARCH

Open Access



Evaluation of photoreceptor-directed fibroblasts derived from retinitis pigmentosa patients with defects in the *EYS* gene: a possible cost-effective cellular model for mechanism-oriented drug

Dilip Rai¹, Masaki Iwanami^{2,6}, Yoriko Takahashi³, Yukari Komuta^{1,7}, Noriyuki Aoi^{4,8}, Akihiro Umezawa⁵ and Yuko Seko^{1*} 

Abstract

Background: The most common gene responsible for autosomal recessive retinitis pigmentosa (RP) is *EYS*. The manner of decay of genetically defective *EYS* gene transcripts varies depending on the type of mutation using our cellular model, which consists of induced photoreceptor-directed fibroblasts from *EYS*-RP patients (*EYS*-RP cells). However, disease-specific profiles have not been clarified in *EYS*-RP cells. Herein we investigated comprehensive gene expression patterns and restoration of altered expression by low molecular weight molecules in *EYS*-RP cells.

Methods: Using induced photoreceptor-like cells by *CRX*, *RAX*, *NeuroD*, and *OTX2*, we employed qRT-PCR and DNA microarray analysis to compare expression levels of disease-related genes in *EYS*-RP cells. We investigated the effect of antiapoptotic or anti-endoplasmic reticulum (ER) stress/antioxidant reagents on the restoration of altered gene expression.

Results: Expression levels of phototransduction-related genes (blue opsin, rhodopsin, S-antigen, GNAT1, GNAT2) were lower in *EYS*-RP cells. *CRYGD* was extracted by global gene expression analysis, as a downregulated, retina-related and apoptosis-, endoplasmic reticulum (ER) stress- or aging-related gene. Pathway enrichment analysis suggested that “complement and coagulation cascades,” “ECM-receptor interaction” and “PI3K-Akt signaling pathway” could be involved in *EYS*-RP-associated pathogenesis. Among the matching/overlapping genes involved in those pathways, *F2R* was suggested as an *EYS*-RP-associated gene. The downregulation of *CRYGD* and *F2R* was completely restored by additional 4-PBA, an inhibitor of ER stress, and partially restored by metformin or NAC. In addition, 4-PBA normalized the expression level of cleaved caspase-3.

Conclusions: Our cellular model may reflect the ER stress-mediated degenerative retina and serve as a pathogenesis-oriented cost-effective rescue strategy for RP patients.

*Correspondence: seko-yuko@rehab.go.jp; yuko.seko@gmail.com

¹ Sensory Functions Section, Research Institute, National Rehabilitation Center for Persons With Disabilities, 4-1 Namiki, Tokorozawa 359-8555, Japan

Full list of author information is available at the end of the article



Keywords: Redirect differentiation, Dermal fibroblast, Photoreceptor, Disease modeling, Retinitis pigmentosa, *EYS*, Semiquantitative analysis, *CRYGD*, *F2R*, ER stress, 4-PBA

Background

Retinitis pigmentosa (RP) is an inherited retinal dystrophy. Defects in the *EYS* gene on chromosome 6q12 are a major cause of autosomal recessive (ar) RP [1–4]. In Japan, defects in the *EYS* gene such as c.4957dupA (p.Ser1653Lysfs*2) and c.8805C>A (p.Tyr2935*) have been identified as pathogenic mutations in about 20–30% of arRP patients [5–9]. Hereafter, arRP caused by defects in the *EYS* gene will be referred to as “EYS-RP.” EYS-RP is characterized as late onset and progressive in severity, leading to visual loss. Therefore, it is an urgent global issue to develop a strategy to delay progressive retinal dystrophy. Although gene therapy has been reported to be safe and effective for one type of inherited retinal dystrophy [10–13], and several drugs are promising [14–17], no established treatments are available for EYS-RP to date.

Because RP patients show heterogenous phenotypes due to heterogeneous gene defects, it may be ideal to determine inhibitory strategies depending on the specific pathogenesis. For this purpose, cellular models are available in place of human retinas. Induced photoreceptor cells derived from iPSCs of RP patients with defects of genes other than the *EYS* gene were reported to reproduce pathogenic phenotypes [18, 19], indicating that the number of rod photoreceptor cells was decreased and that endoplasmic reticulum (ER) stress might be involved. Although methods to generate photoreceptors from iPSCs have been established [20, 21], they are expensive and time-consuming. Another method, transduction of fate-determining transcription factors [22–25], which is called “redirect differentiation,” can produce photosensitive photoreceptor-like cells from somatic cells. Using “redirect differentiation,” we produced photoreceptor-like cells from dermal fibroblasts of EYS-RP patients with homozygous or heterozygous mutations, as a replacement for the degenerative retinas from EYS-RP patients [26]. In that study, we demonstrated that the manners of decay of the *EYS*

gene transcripts varied, depending on type of defect in the *EYS* gene. It was also suggested that defects in the *EYS* gene might be relevant for cell growth rates and that the cell growth rate may be determined mainly by donor age. Therefore, findings in the EYS-RP-derived cells should be compared with those in age-matched control-derived cells for accurate assessment of the characteristics of EYS-RP-derived photoreceptor-like cells.

In the present study, we compared expression levels of phototransduction-related genes (blue opsin, rhodopsin, S-antigen, guanine nucleotide-binding protein G(t) subunit alpha-1 and 2 (GNAT1, GNAT2)) by qRT-PCR and gene expression profiles by microarray in photoreceptor-like cells from EYS-RP patients with those from age-matched normal volunteers. EYS-RP patients showed decreased levels of phototransduction-related genes, consistent with in vivo models reported previously [27]. By global gene expression profiling, *CRYGD* and *F2Y* were downregulated genes in EYS-RP-derived cells. We further investigated whether four drugs, 4-phenyl butyric acid (4-PBA), rapamycin, N-acetyl-L-cysteine (NAC), and metformin, could restore downregulation of these genes. Rapamycin, the inhibitor of mammalian target of rapamycin [28] (mTOR), has been suggested to inhibit photoreceptor degeneration in vivo [29, 30] and in vitro [31]. A well-known chemical chaperone, 4-PBA, is an FDA approved drug for urea cycle disorders owing to its effectiveness in reducing endoplasmic reticulum (ER) stress [32] and was reported to prevent photoreceptor degeneration [14]. The anti-inflammatory drug metformin had shown neuroprotective effect in *rd1* mice [17]. The antioxidant drug NAC suppressed photoreceptor death in *rd10* mice [15]. The present study showed that downregulation of phototransduction-related genes, *CRYGD* and *F2R*, in EYS-RP-derived cells was completely restored by 4-PBA, partially restored by metformin or NAC, but not by Rapamycin.

Table 1 Defects in the *EYS* gene in patients for this study

Patient #	ID	Sex	Age (year)	Allele 1		Allele 2	
				Mutation	Effect	Mutation	Effect
1	RP38	F	67	c.4957dupA	p.Ser1653Lysfs*2	c.4957dupA	p.Ser1653Lysfs*2
2	RP174	M	58	c.4957dupA	p.Ser1653Lysfs*2	c.8805C>A	p.Tyr2935*

Methods

Isolation and culture of dermal fibroblasts

Dermal fibroblasts were harvested from three healthy donors [N#1 (53 years old), N#2 (48 years old), N#3 (63 years old)] and two EYS-RP patients (Pt#1, Pt#2, Table 1) under the approval of the Ethics Committee of the National Rehabilitation Center for Persons with Disabilities (NRCD). These five donors were studied in our previous paper [26]. Signed informed consent was obtained from the donors, and samples were de-identified. All experiments involving human cells and tissues were performed in line with the Declaration of Helsinki. Establishment of fibroblast culture derived from those five donors was performed as previously reported by us [26]. Seventh or eighth-passaged cells were used for following photoreceptor-directed differentiation.

Induction of photoreceptor-like cells (photoreceptor-directed fibroblasts)

Induction experiments were performed as previously reported [23, 24, 26]. In brief, full-length transcription factors, *CRX*, *RAX*, *NeuroD* and *OTX2*, were amplified from cDNAs prepared from total RNA of adult human retina (Clontech, CA, USA) by PCR and cloned into the XmnI-EcoRV sites of pENTR11 (Invitrogen). Preparation and infection with recombinant retrovirus were performed as previously reported [23]. In brief, the resulting pENTR11-transcription factors were recombined with pMXs-DEST by use of LR recombination reactions as instructed by the manufacturer (Invitrogen). The retroviral DNAs were then transduced into 293FT cells, and 3 days later the media were collected and concentrated. The human dermal fibroblasts were infected with this media containing retroviral vector particles as a mixture of the four transcription factors. After the retroviral infection, the media were replaced with the differentiation media, DMEM/F12/B27 medium supplemented with 40 ng/ml bFGF, 20 ng/ml EGF, fibronectin and 1% FBS. The retrovirus-infected cells were cultured for one to six weeks in 6-well or 24-well laminin-coated culture dishes. Expression of the four transgenes (*CRX*, *RAX*, *NeuroD* and *OTX2* (referred to as CRNO)) was confirmed by endpoint RT-PCR, and *CRX* was confirmed by immunocytochemistry in all photoreceptor-directed fibroblasts tested.

Global gene expression analysis

To compare the gene expression profiles in photoreceptor-directed fibroblasts derived from EYS-RP patients with those from normal volunteers, we analyzed the expression levels of 58,201 probes in the induced/non-induced photoreceptor-like cells with or without EYS

genes defects using the SurePrint G3 Human Gene Expression Microarray 8 × 60 K Ver.2.0 (Agilent Technologies, Palo Alto) using total RNA extracted from the cells. To average experimental variations, extracted total RNA samples were pooled into one tube from three independent induction experiments, and pooled samples were subjected to microarray analyses. To normalize the variations in staining intensity among chips, the 75th percentile of intensity distribution was aligned across arrays using GeneSpring software version 12.5 (Agilent). We first compared expression profiles for all the probes and then for refined probes based on GO terms: retina-related and apoptosis, oxidative stress, ER stress or aging (GO (retina) and GO (cell death), respectively). We extracted the intersection of two groups of genes, i.e., up- or downregulated and GO (retina) or GO (cell death)-related genes. For pathway enrichment analysis, WebGestalt2017 (<http://www.webgestalt.org/>) with KEGG pathway (Kyoto Encyclopedia of Genes and Genomes pathway) as a database was used.

Drug administration

The dermal fibroblasts obtained from EYS-RP patients (Pt#1, Pt#2) and age-matched healthy individual (N#3, N#1) were seeded in laminin-coated (Biolamina, 521) 24-well plates. The fibroblasts were transduced with mixture of CRNO as described in the “Induction of photoreceptor-like cells (photoreceptor-directed fibroblasts)” section. After 5–6 h of retroviral transduction, the media in transduced fibroblast cells were replaced with differentiation media containing either one of the four drugs (rapamycin (Selleck chemicals, Cat#S1039), 4-PBA (WAKO, Cat#168-06471), NAC (WAKO, Cat#015-05132), metformin (Abcam, Cat#ab120847)), vehicle or no addition for Pt#1 and containing vehicle or no addition for N#3. Rapamycin was used at the final concentration of 10 nM from the stock solution of 1 M dissolved in 100% ethanol. The 4-PBA was used the concentration of 5 mM from the freshly prepared solution of 5 M 4-PBA in 100% ethanol. A final concentration of 5 mM metformin was prepared from the stock solution of 100 mM metformin in water. Freshly prepared 1 M NAC in water was further diluted to make a final concentration of 5 mM NAC. The media with or without drugs or vehicle was replaced thrice weekly. Finally, the cells were harvested 2 weeks post-transduction. Total RNA was isolated using a Picopure™ RNA isolation kit (Thermo Fisher Scientific; Cat#KIT0204) following the manufacturer’s protocol. cDNAs were synthesized from total RNA using superscript™ IV first-strand synthesis system (Thermo Fisher Scientific; Cat#18091050).

Reverse transcriptase (RT)-PCR

Total RNA was isolated with RNeasy Plus mini kit[®] (Qiagen, Maryland, USA) or PicoPure[™] RNA Isolation Kit (Arcturus Bioscience, CA, USA) according to the manufacturer's instructions. An aliquot of total RNA was reverse-transcribed by using an oligo (dT) primer. A cDNA template was amplified using the Platinum Quantitative PCR SuperMix-UDG with ROX (Invitrogen) and ABI7900HT Sequence Detection System (Applied Biosystems). Fluorescence was monitored during every PCR cycle at the annealing step. The authenticity and size of the PCR products were confirmed using a melting curve analysis (using software provided by Applied Biosystems) and a gel analysis. mRNA levels were normalized using β -actin as a housekeeping gene. The expression level in the photoreceptor-directed fibroblasts, HDF-a (Human Dermal Fibroblasts-adult, ScienCell Research Laboratories), 2 weeks post-transduction was used as a reference. The design of the PCR primer sets is shown in our previous paper [23] and Table S2 (Additional file 2).

Immunocytochemistry

The cells were seeded in laminin-coated 24-well plate (Sumilon MS-92132). The induction of photoreceptor-like cells was carried out mentioned above. The cells were fixed with 4% paraformaldehyde in $1 \times$ PBS 14 days after transduction. The cells were washed and permeabilized with 0.1% Triton in $1 \times$ PBS. The cells were incubated in blocking buffer (5% normal goat serum in $1 \times$ PBS) for an hour at room temperature. The cells incubated with primary antibody (anti-CRX (1:1000, Abnova H00001406-M02), anti-rhodopsin (1D4) (1:200, Santa Cruz biotechnology, sc-57432)) in blocking buffer for overnight at 4C. Then, cells were incubated with secondary antibody (goat anti-mouse IgG, alexa flour[®] 568 conjugate (1:500, Invitrogen, A-11004)). The nuclei were stained with 4',6-diamidino-2-phenylindole (DAPI). Images were captured with a Nikon Eclipse TE300, and contrast and brightness were adjusted with NIS elements AR 3.2.

Western blots

The induced photoreceptor-directed fibroblasts were lysed with radioimmunoprecipitation assay (RIPA) buffer (50 mM tris pH 8.0, 150 mM NaCl, 0.1% sodium dodecyl sulfate, 0.5% sodium deoxycholate and 1% NP40 substitute) containing 1X protease inhibitor cocktail (Roche). The cell lysates were homogenized with gentle agitation for 30 min on ice and centrifuged at 12,000 rpm at 4 °C for 20 min. Each supernatant was collected in a new microcentrifuge tube. The protein concentration of each sample was measured by the Pierce[™] BCA Protein Assay Kit (ThermoScientific). The samples were denatured with

4 X Laemlli sample buffer (Biorad), heated at 95 °C for 5 min, resolved in 4–20% gel (Biorad) and transferred to PDVF membrane (Biorad). Detection of immune complexes formed by proteins of interest and primary antibodies (anti-blue opsin (1:250, Milipore, AB5407), anti-CHOP (1:1500, Cell Signaling Technology, #2895), anti-cleaved caspase-3 (1:1000, Cell signaling technology, #9664), anti- β -actin (1:1000, Cell Signaling Technology)) was performed by enzyme-linked color development with anti-mouse horseradish peroxidase (HRP)-conjugated secondary antibody (1:3000, Cell Signaling Technology). The signals based on chemical luminescence (ECL[™] Prime Western Blotting system (Amersham)) were detected by ChemiStage (TOYOBO). The band intensity was quantified with ImageJ software (National Institutes of Health).

Statistical analysis

Analysis of variance (ANOVA) with Tukey's honest test was employed to compare of the gene expression level of multiple groups with the photoreceptor-directed fibroblasts derived from the healthy individuals (control group). *p* value less than 0.05 was considered significant.

Results

Expression levels of phototransduction-related genes were lower in induced photoreceptor-like cells from fibroblasts of EYS-RP patients

It was previously reported that immunostaining of blue opsin was decreased in EYS-deficient zebrafish [33]. We compared expression levels of phototransduction-related genes, *OPN1SW* (the blue opsin gene), *SAG* (the S-antigen gene), *RCVRN* (the recoverin gene), *RHO* (the rhodopsin gene), *GNAT1* and *GNAT2*. From one to six weeks after CNRO gene transduction, expression levels of the blue opsin gene, the recoverin gene and the GNAT1 gene were lower in photoreceptor-directed fibroblasts derived from EYS-RP patients (Fig. 1). In EYS-RP cells, the lower expression levels of the S-antigen gene initiated 2 weeks after transduction and expression levels were significantly lower 2, 3 and 5 weeks after transduction. Expression levels of the GNAT2 gene were significantly lower one and two weeks after transduction in EYS-RP cells. The expression levels of the rhodopsin gene were lower in EYS-RP cells from one to six weeks, though not significantly (Fig. 1). Expression of blue opsin, rhodopsin and CRX were also detected by immunocytochemistry in photoreceptor-directed fibroblasts derived from both normal healthy volunteers and EYS-RP patients (Additional file 2: Fig. S1, Figure S3 in our previous paper [26]); therefore, statistical analysis was performed on western blots for blue opsin (Additional file 2: Fig. S4).

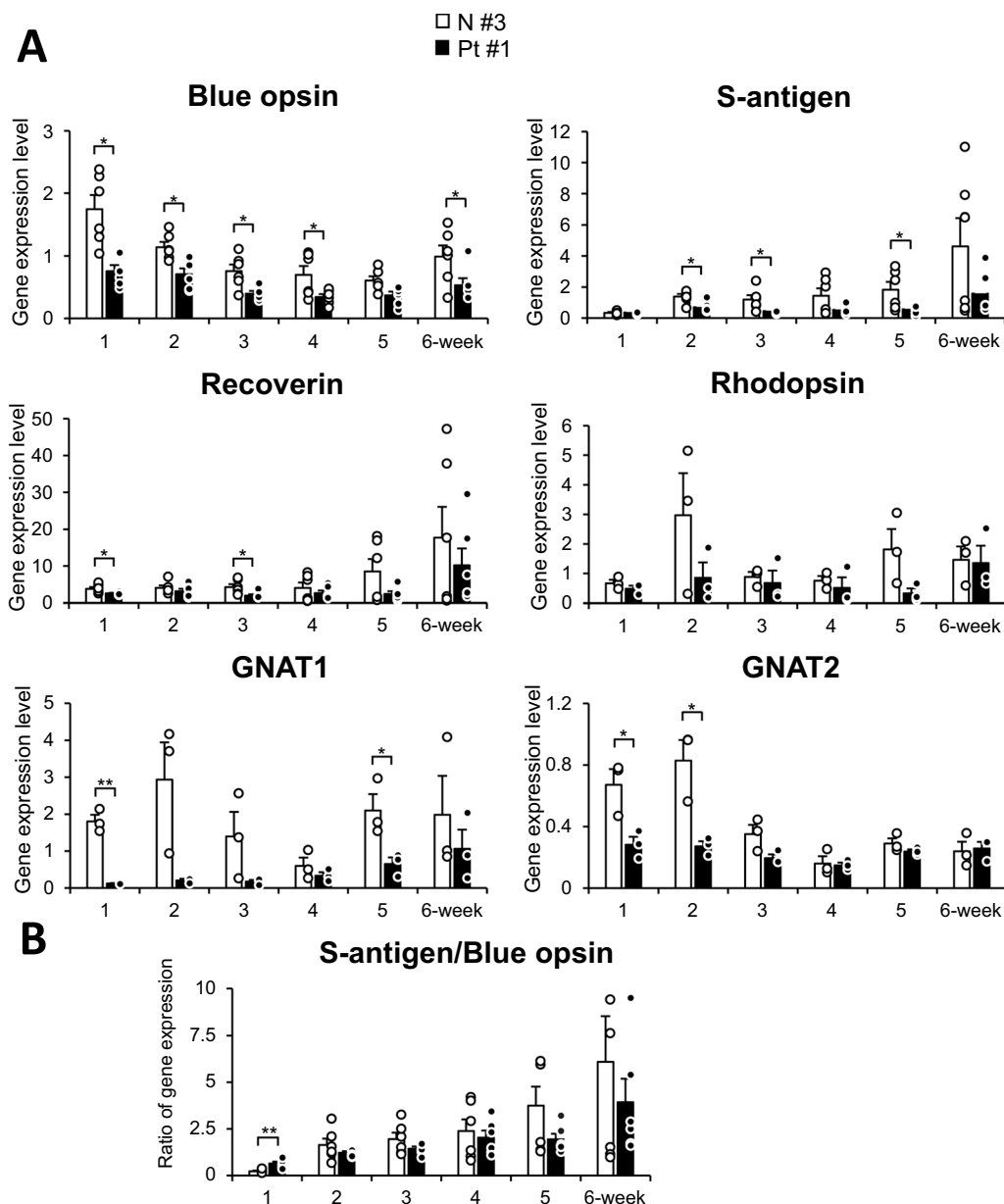


Fig. 1 Induction of retina-specific genes in human dermal fibroblasts derived from a healthy individual (N#3, open box) and an RP patient (Pt#1, closed box) by retroviral infection of genes for transcription factors CRX, RAX, NeuroD and OTX2. **A** RT-PCR analysis for phototransduction-related genes, blue opsin, S-antigen, rhodopsin, GNAT1, GNAT2, recoverin, in cultured human dermal fibroblasts (HDF). Vertical axis; relative expression, Horizontal axis; weeks after transduction. Columns represent mean \pm SEM. All data points are overlaid. ** $p < 0.01$; student's t-test ($n = 6$ (blue opsin, S-antigen, recoverin), $n = 3$ (GNAT1, GNAT2)). **B** Ratio of expression levels of rod photoreceptor- and cone photoreceptor-specific genes in photoreceptor-like cells (S-antigen vs blue opsin). Error bar: SEM. ** $p < 0.01$; student's t-test ($n = 6$)

NRL, a key transcription factor for rod differentiation, was downregulated gene in the photoreceptor-directed fibroblasts derived from EYS-RP patients

To clarify the specific gene expression profiles in induced photoreceptor cells derived from EYS-RP patients, we compared the expression profiles of 58,201 probes in

the induced photoreceptor cells derived from EYS-RP patients (induced, RP) and healthy volunteers (induced, normal). We first extracted the intersection of the two groups of genes, i.e., up- or downregulated genes in RP versus healthy ([induced Pt#1] versus [induced N#3], which is an age-matched pair for comparison) (signal

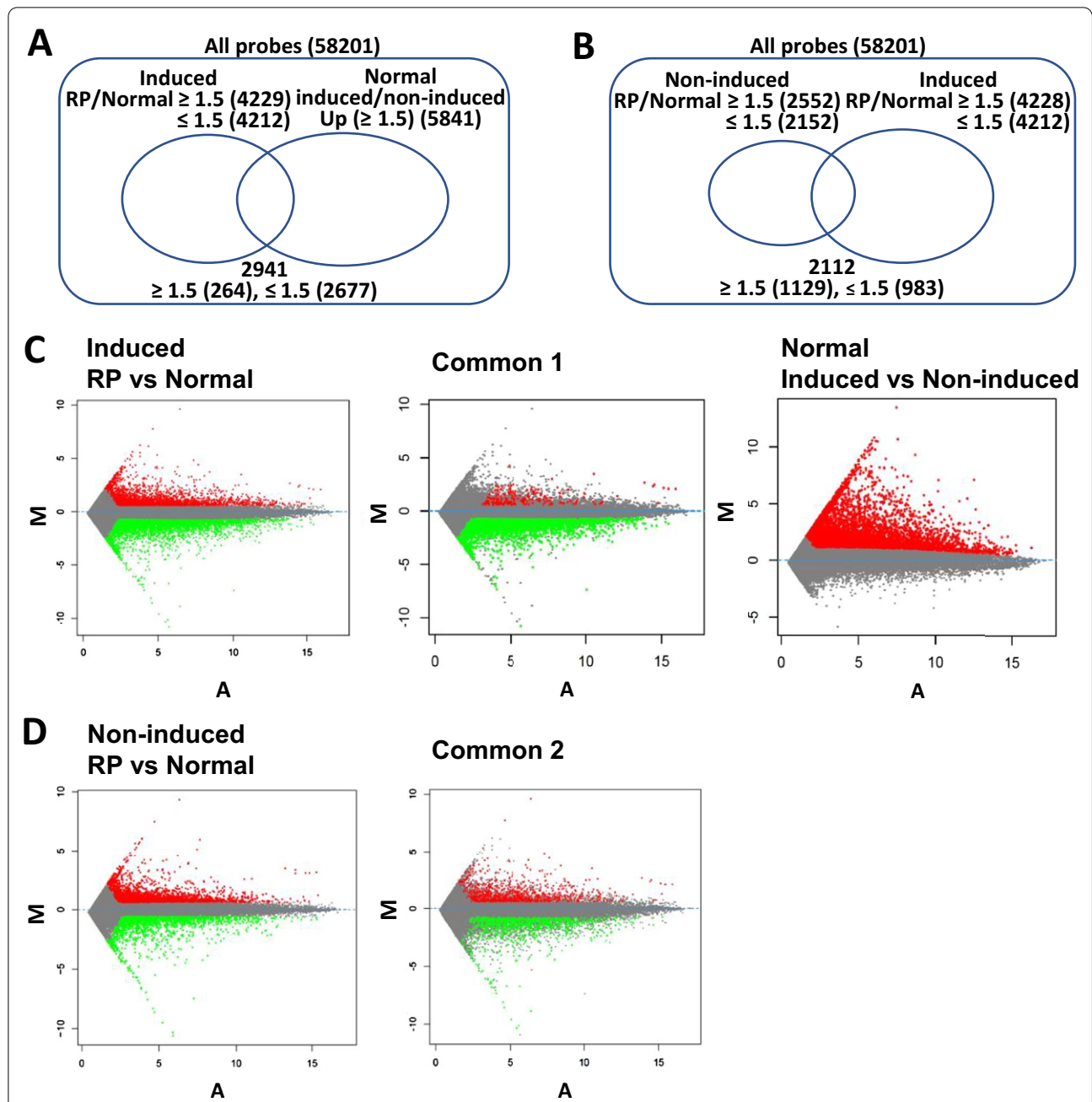


Fig. 2 Categorization of genes that are differentially expressed in photoreceptor-directed fibroblasts derived from an EYS-RP patient and upregulated by transduction of *CRX*, *RAX*, *NeuroD* and *OTX2*. Venn diagrams (A, B) and Mean-average (MA) plots (C, D) to compare EYS-RP cells vs normal cells. To clarify the specific gene expression profile in induced photoreceptor cells derived from EYS-RP patients, we compared the expression profiles of 58,201 probes in the induced photoreceptor cells or non-induced fibroblast cells derived from an EYS-RP patient (induced or non-induced, RP, Pt#1) and healthy volunteers (induced or non-induced, normal, N#3), using microarrays. We first extracted the intersection of the two groups of genes, i.e., up- or downregulated genes in RP versus healthy ([induced Pt#1] versus [induced N#3], which is an age-matched pair for comparison) (signal ratio $\geq +1.5$, ≤ -1.5 for “up,” “down”) and those in CRNO-transduced normal fibroblasts versus non-induced fibroblasts ([induced N#3] versus [non-induced N#3]) (signal ratio $\geq +1.5$) (A). Furthermore, we compared non-induced EYS-RP-derived cells and non-induced normal cells, and then extracted the intersection of the two groups to define up- or downregulated genes (non-induced Pt#1) versus [non-induced N#3]). We also determined up- or downregulated genes in induced RP versus induced healthy ([induced Pt#1] versus [induced N#3]) (signal ratio $\geq +1.5$, ≤ -1.5) (B). Mean-average (MA) plots indicate differential gene expression between induced RP and induced normal (C) and differential gene expression between non-induced RP and non-induced normal (D). Significantly differentially upregulated genes (signal ratio $\geq +1.5$) are highlighted in red and downregulated genes (signal ratio ≤ -1.5) are highlighted in green

ratio $\geq +1.5$, ≤ -1.5 for “up,” “down”) and those in CRNO-transduced normal fibroblasts versus non-induced fibroblasts ([induced N#3] versus [non-induced N#3]) (signal ratio $\geq +1.5$). A total of 264 upregulated genes and 2677 downregulated genes were extracted, which suggest that there are more downregulated genes in the photoreceptor-directed fibroblasts derived from EYS-RP patients compared to those from normal controls (Fig. 2). Among the 2677 downregulated genes, 50 genes were significantly decreased in another independently performed microarray analysis using independently differentiated photoreceptor-directed fibroblasts (Pt#1 vs N#2), which is an age-unmatched pair (Table 2). Among the genes whose expression levels were greatly decreased, *NRL*, a key transcription factor for rod differentiation, was extracted. We then compared non-induced EYS-RP-derived cells and non-induced normal cells. It was shown that there were more differentially expressed genes, EYS-RP vs normal, in the differentiated experimental groups (4229 upregulated probes, 4212 downregulated probes) (Fig. 2A) than in the non-induced groups (2552 upregulated probes, 2152 downregulated probes) (Fig. 2B).

***CRYGD* was downregulated in EYS-RP-derived cells, retina-related and apoptosis/oxidative stress/ER stress/aging-related genes**

We then extracted intersection of the two groups of genes, i.e., up- or downregulated genes in RP versus healthy and retina-related genes with gene ontology (GO) term annotation, which was used in our previous study [24]. A total of 119 upregulated genes and 239 downregulated genes were extracted, which suggests that there are downregulated genes in RP retinas (Fig. 3). *CNGA1*, *COL11A1*, *SOX11*, *AIPL1* and *CRYGD* showing the largest decreases in expression. We then extracted the interaction of the two groups of genes, i.e., up- or downregulated genes in RP versus healthy and apoptosis/oxidative stress/ER stress/aging-related genes according to gene ontology (GO) term annotation. Those four key words were chosen based on previous studies of animal models of RP [34–37] and the fact that EYS-RP is late-onset and progressive disease. Ninety-six upregulated genes and 146 downregulated genes were extracted, with *CRYGD* and *GJB2* showed the largest decreases in expression. Decreased expression of *CRYGD* in EYS-RP-derived cells was confirmed by qRT-PCR.

F2R may be involved in an EYS-RP-specific pathway

We then prepared a gene set for pathway enrichment analysis, an intersection of up- or downregulated genes in RP versus age-matched healthy ([induced Pt#1] versus [induced N#3]), and another intersection of up- or downregulated genes in RP versus age-unmatched healthy

([induced Pt#1] versus [induced N#2]). Using WebGestalt, we found that three pathways, “complement and coagulation cascades,” “ECM-receptor interaction” and “PI3K-Akt signaling pathway,” were extracted from up- or downregulated genes in photoreceptor-directed fibroblasts derived from EYS-RP compared to normal volunteers. Among the matching/overlapping genes in the three pathways, the *F2R* gene was found in both “complement and coagulation cascades” and “PI3K-Akt signaling pathway.” Decreased expression of *F2R* in EYS-RP-derived cells was confirmed by qRT-PCR.

Decreased expression levels of the phototransduction-related genes, *OPN1SW* (blue opsin), *RCVRN* (recoverin), *GNAT1* and *GNAT2*, and the genes extracted by global gene expression analysis, *GRYGD* and *F2R*, in EYS-RP-derived cells were increased by the chemical chaperone 4-PBA

We tested whether drugs would increase levels of gene expression in photoreceptor-directed fibroblasts derived from EYS-RP to similar levels of those from normal volunteers. Six target genes whose expression levels were decreased in EYS-RP derived cells were chosen (blue opsin, recoverin, *GNAT1*, *GNAT2*, *F2R* and *CRYGD*), based on previous results in the present study. The effectiveness of four drugs was evaluated. 4-PBA was found to be the most effective. The treatment of photoreceptor-directed fibroblasts derived from Pt#1 with 5 mM 4-PBA restored the expression levels of target genes to levels similar to the control group, or higher than the control (N#3) (Fig. 4, Additional file 2: Fig. S2). The gene expression levels with 4-PBA treatment were significantly higher than those of photoreceptor-like cells with a vehicle, EtOH (one-way ANOVA followed by Tukey’s test). The restoration effect by 4-PBA treatment was confirmed by western blotting for the blue opsin (Additional file 2). Similarly, three doses of 4-PBA were tested to determine whether expression levels of the target genes in photoreceptor-directed fibroblasts derived from Pt#2 were also restored to levels of the control (N#1) (Additional file 2: Fig. S3). The application of metformin also increased the expression levels of target genes to comparable or higher levels than the control. However, metformin was less effective in restoring the expression of target genes in photoreceptor-directed fibroblasts derived from Pt#2 (Fig. S3). This discrepancy in effectiveness of metformin might be due to the difference in the point mutation in *EYS* between Pt#1 and Pt#2; however, more samples are needed to clarify this discrepancy. Application of rapamycin and NAC did not restore the expression level of any target genes in photoreceptor-directed fibroblasts derived from Pt#1 to similar levels of the control (N#3) (Fig. 4), as well as Pt#2 versus N#1 (Fig. S3). The

Table 2 Downregulated genes in EYS-RP-derived photoreceptor-like cells

GeneSymbol	GeneName	Pt #1 non-induced (1)	Pt #1 induced (1)	N #3 non-induced (1)	N #3 induced (1)	Pt #1 non-induced (2)	Pt #1 induced (2)	N #2 non-induced (2)	N #2 induced (2)
LZTS1	Leucine zipper, putative tumor suppressor 1	3.24	5.45	5.39	9.43	2.81	5.24	2.98	6.85
SST	Somatostatin	1.00	4.40	1.11	8.27	2.89	4.29	2.27	8.05
TNNC1	Troponin C type 1 (slow)	3.42	4.27	3.68	7.76	2.70	4.39	2.98	7.01
FOXS1	Forkhead box S1	1.66	3.84	1.76	7.07	1.07	4.16	1.94	6.00
ANO2	Anoctamin 2, calcium activated chloride channel	1.48	4.51	2.48	7.60	1.78	4.58	1.86	6.31
HES6	Hes family bHLH transcription factor 6	2.03	4.08	2.28	7.15	3.11	5.29	3.23	6.47
NLRP12	NLR family, pyrin domain containing 12	0.79	3.12	0.93	6.10	1.19	3.17	0.29	6.42
KRT18	Keratin 18, type I	1.63	4.02	4.34	6.90	2.40	3.67	3.05	6.57
HES6	Hes family bHLH transcription factor 6	7.15	10.31	7.33	13.15	7.54	10.83	8.04	12.32
CKMT1A	Creatine kinase, mitochondrial 1A	1.11	6.16	1.17	8.82	1.67	5.82	1.42	7.10
DIRAS3	DIRAS family, GTP-binding RAS-like 3	3.06	3.93	3.94	6.52	2.75	3.79	3.05	5.96
DIRAS3	DIRAS family, GTP-binding RAS-like 3	4.08	7.61	5.35	10.11	4.10	8.07	4.62	9.89
PDLIM3	PDZ and LIM domain 3	2.93	5.31	4.28	7.78	0.59	4.16	0.50	5.70
C8orf46	Chromosome 8 open reading frame 46	2.37	5.04	2.69	7.47	1.08	5.38	1.02	7.36
ASMT	Acetylserotonin O-methyltransferase	3.27	3.88	3.05	6.28	1.92	4.36	1.47	7.99
COL4A1	Collagen, type IV, alpha 1	5.41	7.26	6.24	9.66	6.17	7.64	6.19	9.59
LYPD1	LY6/PLAUR domain containing 1	4.31	5.37	5.84	7.73	4.45	5.13	3.44	7.71
C2CD4A	C2 calcium-dependent domain containing 4A	0.52	6.08	0.51	8.36	1.21	5.85	2.08	7.60
NRL	Neural retina leucine zipper	3.15	8.05	2.60	10.31	2.86	8.76	1.91	10.17
COL4A2	Collagen, type IV, alpha 2	8.89	10.43	9.70	12.66	9.76	10.68	9.49	12.02

Table 2 (continued)

GeneSymbol	GeneName	Pt #1 non-induced (1)	Pt #1 induced (1)	N #3 non-induced (1)	N #3 induced (1)	Pt #1 non-induced (2)	Pt #1 induced (2)	N #2 non-induced (2)	N #2 induced (2)
NRL	Neural retina leucine zipper	4.04	8.84	4.12	11.06	3.83	9.51	3.46	11.02
LINC00463	Long intergenic non-protein coding RNA 463	0.84	4.19	0.96	6.34	0.85	4.35	0.45	6.09
ADRA2A	Adrenoceptor alpha 2A	4.64	7.20	4.12	9.27	4.29	7.40	3.74	8.79
NTRK3	Neurotrophic tyrosine kinase, receptor, type 3	2.36	2.14	0.59	4.06	1.04	3.06	1.54	5.67
NGFR	Nerve growth factor receptor	0.55	4.51	0.60	6.43	0.55	4.91	0.50	7.60
MPPED2	Metallophosphoesterase domain containing 2	0.65	5.29	0.82	7.18	0.37	5.64	0.33	7.84
AMER2	APC membrane recruitment protein 2	0.78	8.01	0.80	9.76	0.68	7.97	1.49	9.80
CTSH	Cathepsin H	6.82	7.64	7.24	9.36	6.46	7.30	6.02	9.51
PDZD2	PDZ domain containing 2	2.19	6.21	2.38	7.92	0.39	6.33	0.99	8.45
TCF15	Transcription factor 15 (basic helix-loop-helix)	6.12	5.76	6.57	7.45	5.49	5.57	5.53	6.92
F2R	Coagulation factor II (thrombin) receptor	2.38	4.05	2.99	5.68	3.10	4.80	3.53	6.61
GRAMD1C	GRAM domain containing 1C	5.88	7.06	6.06	8.62	4.88	7.00	4.46	8.98
GPX3	Glutathione peroxidase 3 (plasma)	4.82	8.34	5.16	9.87	4.60	8.44	3.98	10.67
BEGAIN	Brain-enriched guanylate kinase-associated	4.33	4.39	5.47	5.92	4.45	4.63	4.82	6.59
TMEM176A	Transmembrane protein 176A	3.66	9.80	3.69	11.31	4.13	10.15	4.75	11.75
A2M	Alpha-2-macroglobulin	7.24	5.96	8.35	7.45	8.67	6.78	9.16	8.00
TMSB15A	Thymosin beta 15a	4.54	4.05	5.37	5.51	3.62	4.14	4.51	5.85
GPRC5B	G protein-coupled receptor, class C, group 5, member B	3.92	7.32	3.45	8.77	4.13	7.61	3.75	10.06

Table 2 (continued)

GeneSymbol	GeneName	Pt #1 non-induced (1)	Pt #1 induced (1)	N #3 non-induced (1)	N #3 induced (1)	Pt #1 non-induced (2)	Pt #1 induced (2)	N #2 non-induced (2)	N #2 induced (2)
IMPG1	Interphotoreceptor matrix proteoglycan 1	0.60	4.33	0.56	5.74	0.54	3.93	0.43	6.05
PLEKHB1	Pleckstrin homology domain containing, family B (evectins) member 1	4.54	7.65	4.43	9.05	4.63	7.46	3.97	9.67
SYPL2	Synaptophysin-like 2	7.12	7.76	6.99	9.15	6.21	7.72	5.26	9.92
SLC16A3	Solute carrier family 16 (monocarboxylate transporter), member 3	11.28	11.44	13.32	12.77	13.11	11.60	14.03	12.88
CBX2	Chromobox homolog 2	2.08	5.02	1.71	6.21	3.61	5.17	3.52	6.36
CCDC13	Coiled-coil domain containing 13	2.07	6.52	2.39	7.66	1.83	7.00	1.92	8.75
MECOM	MDS1 and EVI1 complex locus	4.27	3.93	4.27	5.06	3.67	3.40	4.43	5.65
RXRG	Retinoid X receptor, gamma	0.69	6.30	0.72	7.40	0.42	6.87	0.39	8.48
CCDC181	Coiled-coil domain containing 181	3.07	8.39	3.76	9.48	3.08	8.35	3.84	9.70
GNB3	Guanine nucleotide binding protein (G protein), beta polypeptide 3	3.90	6.99	3.99	8.06	3.62	7.18	4.42	8.70
OXTR	Oxytocin receptor	6.26	7.83	5.87	8.86	4.82	7.44	4.35	9.65
		4.79	4.45	5.12	5.46	3.95	4.72	4.92	6.30

expression levels of these genes in photoreceptor-like cells derived from fibroblast of Pt#1 treated with vehicle (water or ethanol) were lower than in control group, however, not significantly (Fig. 4, one-way ANOVA followed by Tukey's test). A similar trend in reduction in the expression level of target genes was also observed in photoreceptor-directed fibroblasts derived from Pt#2, with a heterozygous mutation in the *EYS* gene, and an age-matched healthy individual (N#1) (Fig. S3).

Based on the above results with 4-PBA, we investigated UPR-signal transduction in *EYS*-deficient cellular models. Inositol requiring enzyme 1 α/β (IRE1) is the one of

the key UPR signal activator proteins [38–40]. Thus, we examined the relative expression of *ERN* (endoplasmic reticulum to nucleus signaling), which codes for IRE1. We found that the relative expression of *ERN* was significantly lower in photoreceptor-directed fibroblasts derived from Pt#2 and was also lower in that from Pt#1, although not significantly (Additional file 2: Fig. S4). Treatment with 5 mM 4-PBA restored the relative expression levels of *ERN* in photoreceptor-directed fibroblasts derived from both patients to similar levels a found in healthy individuals (Fig. S4). CHOP (C/EBP homologous protein) is one of the target genes of the UPR pathway

and has a role in controlling gene expression that leads to apoptosis [38–40]. We examined the expression level of CHOP by western blotting, using photoreceptor-directed fibroblasts derived from Pt#1 and N#3. CHOP was undetectable in both fibroblasts. Upon treatment with thapsigargin (200 mM), an ER stress inducer, the expression levels of CHOP were slightly higher in Pt#1-derived cells than N#3, albeit statistically insignificant (Fig. S4). We performed western blotting with a cleaved caspase-3 antibody to investigate the restoration effect of 4-PBA on apoptosis. The relative expression of cleaved caspase-3 was slightly higher in EYS-RP than photoreceptor-like cells derived from a healthy individual, although there was no significant difference. The relative expression of cleaved caspase-3 was clearly decreased by 4-PBA treatment. By immunostaining, caspase-3 was also detected in more photoreceptor-directed fibroblasts derived from Pt#1 rather than N#3 under thapsigargin supplementation (Additional file 2: Fig. S5). These results indicate that EYS-RP-derived cells are more sensitive to an ER stress inducer.

Discussion

This is the first report that shows gene expression profiles of cellular models of EYS-RP patients. Because our previous study suggested that findings of patient-derived cells should be compared with age-matched normal volunteer to assess EYS-RP-associated characteristics [26], we here compared gene expression profiles in induced photoreceptor-directed fibroblasts derived from EYS-RP patients with age-matched normal volunteers. As a result, expression levels of several phototransduction-related genes, blue opsin, recoverin, GNAT1, GNAT2, and an aging-related gene, *CRYGD*, and complement and coagulation cascades- and PI3K-Akt signaling pathway-related gene, *F2R*, were significantly lower in photoreceptor-directed

fibroblasts derived from EYS-RP patients compared to age-matched normal volunteers. This decrease was reversed by addition of 4-PBA and metformin, but not by rapamycin or NAC.

One of the downregulated genes, the γ D-crystallin encoding *CRYGD* gene, which was extracted as both retina-related and apoptosis/oxidative stress/ER stress/aging-related genes (Fig. 3), is also known as a cataractogenesis-related gene [41]. On the other hand, *SLC16A10* (*LAT2*), which is also a cataractogenesis-related gene [42], was extracted by pathway enrichment analysis as involved in the “protein digestion and absorption pathway” (Additional file 1: Table S1), in the intersection of up- or downregulated genes in RP versus age-matched healthy volunteer and those in CRNO-transduced normal fibroblasts versus non-induced fibroblasts. RP, most likely including EYS-RP, is a typical late-onset retinal degenerative disease, with cataract formation noted at relatively younger ages [43–45]. The mechanism for pathologic, not physiological, aging-related cataractogenesis in EYS-RP has not been elucidated; however, it may be explained, at least in part, by downregulation of the *CRYGD* gene in photoreceptors of EYS-RP patients. Furthermore, crystallin plays roles outside of the lens, with cilia-related functions in photoreceptors [46]. Of note, defects in human γ D-crystallin, known to form amyloid aggregates, were suggested to play a role in retinal pigment epithelial cells, leading to age-related macular degeneration [47]. Our results suggest possible roles of downregulated γ D-crystallin in EYS-associated photoreceptor degeneration as well as cataractogenesis. In the present study, Gap junction protein, beta 2 (*GJB2*) showed decreased expression by the same analysis. The *GJB2* gene, which encodes connexin 36, was reported to be related to myopia development [48]. It is also known that *GJB2* plays a role in retinal

(See figure on next page.)

Fig. 3 Global gene expression analysis of EYS-RP patient-derived photoreceptor-like cells. **A** Categorization of genes differentially expressed in both photoreceptor-directed fibroblasts derived from an EYS-RP patient and retina-related genes. We extracted intersection of the two groups of genes, i.e., up- or downregulated genes in RP versus healthy and retina-related genes according to gene ontology (GO) term annotation, which was used in our previous study [24]. A total of 119 upregulated genes and 239 downregulated genes were extracted (left panel). *NGA1*, *COL11A1*, *SOX11*, *AIP1* and *CRYGD* showed significant decreases in expression (Right panel). **B** Categorization of genes that are both differentially expressed in photoreceptor-directed fibroblasts derived from an EYS-RP patient and apoptosis/oxidative stress/ER stress/aging-related genes according to gene ontology (GO) term annotation. Ninety-six upregulated genes and 146 downregulated genes were extracted, with *CRYGD* and *GJB2* displaying large decreases. **C** EYS-RP-associated pathway extracted by pathway enrichment analysis. Pathway enrichment analysis was performed on a gene set that is an intersection of up- or downregulated genes in RP versus age-matched healthy ([induced Pt#1] versus [induced N#3]), and another intersection of up- or downregulated genes in RP versus age-unmatched healthy ([induced Pt#1] versus [induced N#2]), which was served for the analysis. By pathway enrichment analysis, WebGestalt2017 (<http://www.webgestalt.org/>), three pathways, “complement and coagulation cascades,” “ECM-receptor interaction” and “PI3K-Akt signaling pathway,” were extracted from up- or downregulated genes in photoreceptor-directed fibroblasts derived from EYS-RP compared to normal volunteers. Among the matching/overlapping genes in the three pathways, the *F2R* gene was involved in both the “complement and coagulation cascades” and “PI3K-Akt signaling pathway.” **D** RT-PCR analysis of expression of *CRYGD* and *F2R* genes in photoreceptor-directed fibroblasts derived from an EYS-RP patient (Pt#1) and a normal volunteer (N#3). The vertical axis is relative expression, and the horizontal axis is weeks after gene transduction. Decreased expression of *CRYGD* and *F2R* in EYS-RP-derived cells was confirmed. The expression levels in photoreceptor-directed fibroblasts transduced with four transcription factor genes (*CRX*, *RAX*, *NeuroD* and *OTX2*) was calculated from 3 biological replicates. Columns represent mean \pm SEM. All data points are overlaid. * $p < 0.05$, ** $p < 0.01$; student's t-test. Internal control: β -actin.

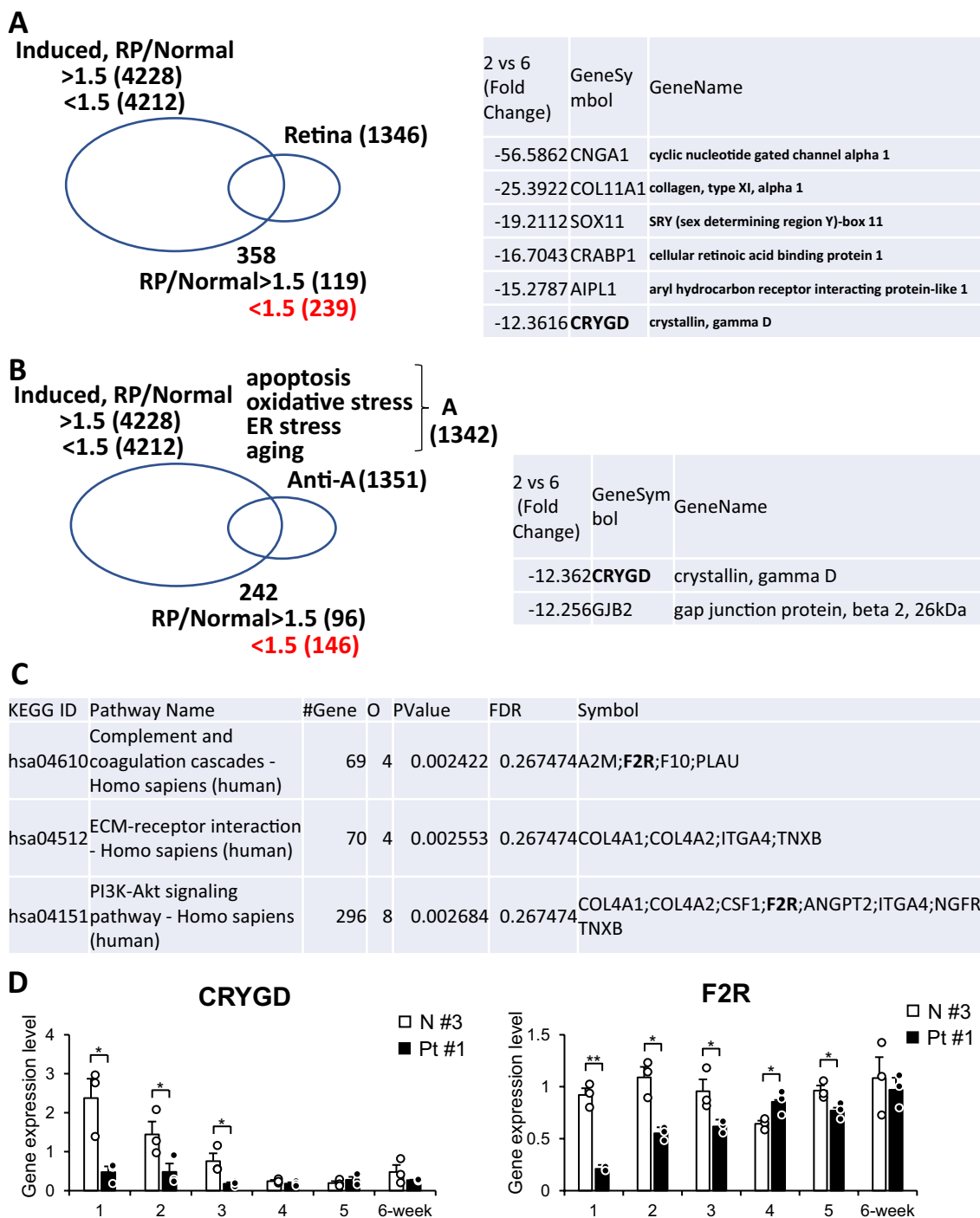


Fig. 3 (See legend on previous page.)

signal transduction and is expressed in gap junctions between cones, rods and bipolar cells, playing essential roles in rod-mediated visual signals [49, 50]. Further studies are needed to clarify the molecular interactions of CRYGD and GJD2 with EYS in the retina.

EYS, an agrin/perlecan-related extracellular matrix protein secreted by photoreceptors into the interphotoreceptor or subretinal space of the human retina. A recent report supports the possible function of

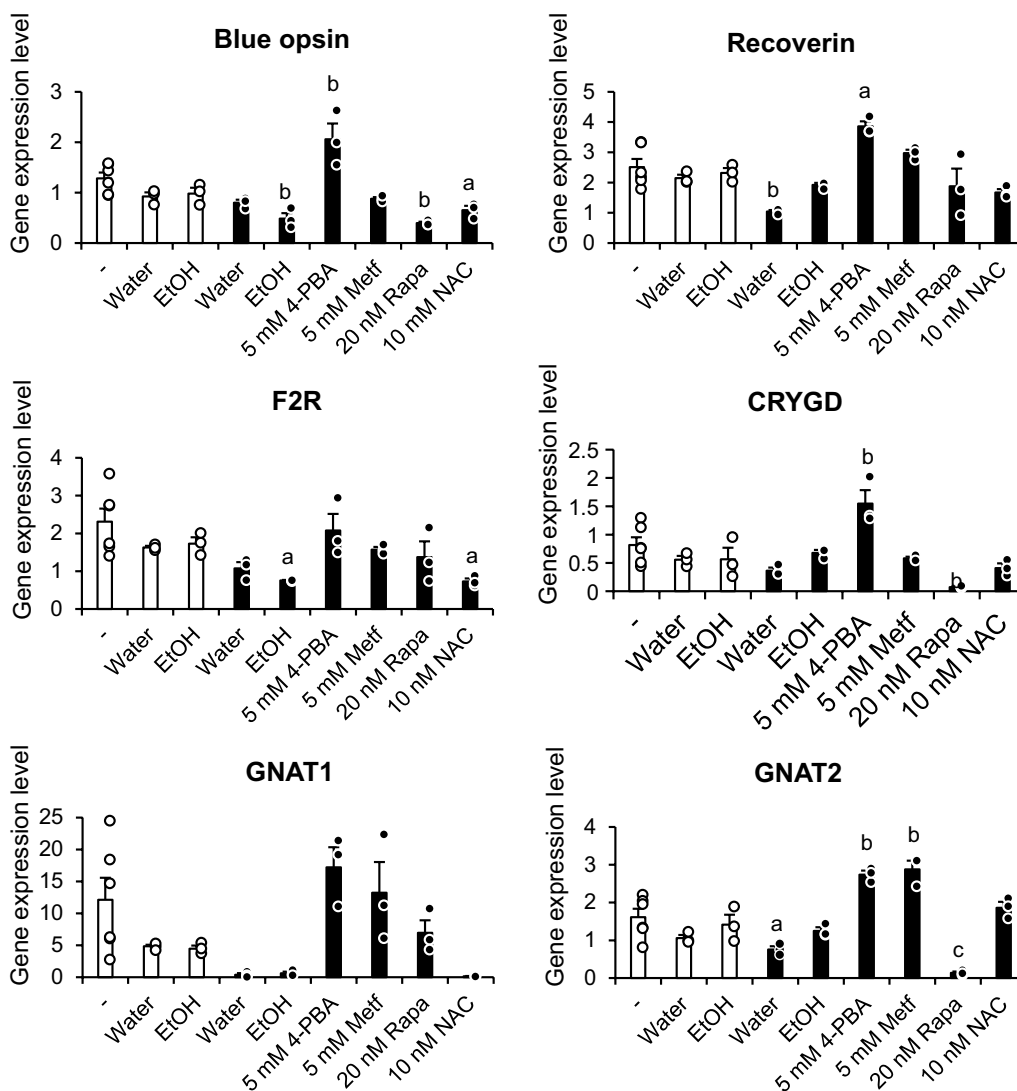


Fig. 4 Effect of drugs on gene expression in photoreceptor-directed fibroblasts derived from an EYS-RP patient, Pt#1. The fibroblasts of a healthy individual (N#3) and fibroblasts of a patient suffering from retinitis pigmentosa due to a homozygous mutation in the *EYS* gene (Pt#1) were transdifferentiated to photoreceptor-like cells by retroviral transduction of four transcription factors. Gene expression was compared 2 weeks post-transduction. Differentiation medium was supplemented with four drugs, 4-phenylbutyric acid (4-PBA), metformin (Metf), rapamycin (Rapa), N-acetyl-L-cysteine (NAC) or the vehicle (water and ethanol (EtOH)) or none (-). The gene expression with each pharmacological treatment was compared to the gene expression in photoreceptor-like cells derived from fibroblasts of healthy individual without any supplement (-). Columns represent mean \pm SEM. All data points are overlaid ($n=6$ (N#3 without any supplement (-)), $n=3$ (N#3 with supplement and Pt#1)). $a=p>0.05$, $b=p>0.01$, $c=p>0.001$; One-way ANOVA followed by Tukey's honest test. For the sake of simplicity, comparison with the gene expression level in N#3 without any supplement (-) is shown here. Comparison among other groups is shown in Additional file 2: Fig. S2

EYS as an extracellular matrix protein in the retina of a zebrafish model with defects in the *eyes* gene [52]. From our present study using a human cellular model of EYS-RP, interphotoreceptor matrix proteoglycan 1 (IMPG1) (Table 2) and ECM-receptor interaction pathway (Fig. 3, Table S1) were extracted as an EYS-RP-associated gene and pathway, suggesting the ECM-related functions of EYS throughout evolution.

On the other hand, in previous reports using zebrafish, the EYS protein is localized near connecting cilium/transition zone in photoreceptors [27, 32, 53] and disruption of the ciliary pocket in cones is observed in *eyes*^{-/-} [32]. The study further showed that expression of opsin, localized in outer segment of photoreceptors, is extremely lower in *eyes*^{-/-}, and the authors speculate that the lower expression is due to disruption of transport in cilia. We

here show that expression levels of several phototransduction-related genes, blue opsin, recoverin, GNAT1, GNAT2 were significantly lower in photoreceptor-directed fibroblasts derived from EYS-RP patients compared to age-matched normal volunteers. A regulatory mechanism other than transportation via connecting cilium may exist in EYS deficiency because our photoreceptor-like cells lack outer segments, although gathering mitochondria were observed [23]. On the other hand, Nrl, a key molecule to control rod-photoreceptor development [54, 55], was extracted as one of the significantly downregulated genes in EYS-RP derived cells in this study (Table 2). This may lead to the typical phenotype of RP or EYS-RP, rod-cone dystrophy [56, 57], although atypical phenotypes of RP, such as cone/cone-rod dystrophy and sector RP, have been reported [58–60]. It is also noteworthy that expression levels of blue opsin and the ratio of expression levels of blue opsin vs S-antigen were significantly lower in the earlier days after CRNO gene transduction in EYS-RP-derived photoreceptor-like cells, which may be explained by the fact that up-regulation of cone-photoreceptor-related genes, started earlier than rod-photoreceptor genes [23], which are consistent with previous reports on retinogenesis. In our redirect differentiation study, it is difficult to discern whether downregulation of phototransduction-related genes is related to delay, defects of retinogenesis or decrease of differentiation efficiency in EYS-RP cells. Correlation of gene expression profiles to phenotype should be helpful, as well as genotype–phenotype relation for personalized medicine.

Pathway enrichment analysis revealed that three pathways were extracted from differentially expressed genes between EYS-RP and normal volunteers (Fig. 3). In those pathways, *F2R*, which encodes protease-activated receptor-1 (PAR-1), was matching/overlapping in both “complement and coagulation cascades” and “PI3K-Akt signaling pathway.” Decreased expression of the *F2R* gene in EYS-RP-derived cells was confirmed by qRT-PCR (Fig. 3). Those pathways and the *F2R* gene may be promising as therapeutic targets because there is evidence of the involvement of inflammation in the pathogenesis of RP [61–64]. *F2R* may also be involved in prevention of apoptosis [65], morphogenesis of photoreceptors [66] and survival of cancer cells through a Bcl-xL-dependent mechanism [67]. Reduction of *F2R* expression by defects in the EYS gene may be relevant to multiple cascades in EYS-RP.

It was reported that a defect in the rhodopsin gene, P23H, the most common cause of RP in the USA, induces rhodopsin misfolding and the unfolded protein response (UPR) [36]. Also, it was shown that the endoplasmic reticulum (ER)-UPR, a known mechanism of apoptosis

secondary to an overwhelming accumulation of misfolded protein [68], is involved in photoreceptor degeneration caused by missense mutations in TULP1 [69], which are associated with two forms of IRDs, early-onset retinitis pigmentosa (RP) and Leber congenital amaurosis (LCA). In this study, we demonstrated that 4-phenylbutyric acid (4-PBA), chemical chaperone, an ER stress inhibitor, dramatically restored downregulation of phototransduction-related genes, *CRYGD* and *F2R*, suggesting that ER stress may be a possible therapeutic target for photoreceptor degeneration in EYS-RP patients.

In our previous paper, we demonstrated that the defective *EYS* mRNA containing c.4957dupA in photoreceptor-directed fibroblasts of Pt#1 and Pt#2 undergoes partial degradation [26]. In the present study, we show that the expression level of *ERN*, which codes IRE1, was decreased in photoreceptor-directed fibroblasts derived from Pt#1 and Pt#2. It is well established that IRE1 degrades mRNA via RIDD (regulated Ire1-dependent decay) pathway to mitigate ER stress [38–40]. The failure to degrade faulty mRNA in EYS-RP might be attributable to lowered expression of ERN. IRE1 has also been reported to promote secretion of Spacemaker/Eyes shut in the intrarhabdomeral space in *Drosophila* [70]. This could be one of the reasons for depletion of IRE1 expression. Additionally, IRE1 is reported to play a role in photoreceptor differentiation via RIDD pathway [70]. We speculate the decreased level of IRE1 might be due to the reduced protein translation in response to ER stress. It is plausible that the depletion of IRE1 might have affected the redirect differentiation in EYS-RP, thereby causing a decrease in expression levels of phototransduction-related genes. We are planning additional detailed studies on mRNA degradation by the RIDD pathway to clarify the abovementioned hypothesis. Our study also showed that the 4-PBA effectively restored the expression levels of *ERN* in EYS-RP-derived induced cells to levels similar of healthy individuals. Apparently, 4-PBA may attenuate the ER stress by various mechanisms. One plausible mechanism of 4-PBA-mediated upregulation of several EYS-RP-associated genes might be due to upregulation of *ERN*, thereby possibly promoting mRNA degradation of defective *EYS* mRNA or facilitating the redirect differentiation to photoreceptors. To clarify this speculation, further studies are needed.

By our pathway enrichment analysis using microarray data of EYS-RP-patient-derived photoreceptor-like cells, “hypertrophic cardiomyopathy (FDR: 0.011684)” and “dilated cardiomyopathy (FDR: 0.014503)” were extracted (Table S1). It was suggested that EYS protein in *Drosophila* plays a role in protecting mechanoreceptor and chemoreceptor organs from hyperosmotic shock by providing stiffness and maintaining cellular integrity

and tissue morphogenesis [71]. A genetic study suggested an association between trastuzumab-induced cardiotoxicity and rs139944387 in exon 44 of Eyes shut homologs [EYS] [72]. On the other hand, in *Drosophila*, localization and function of actomyosin machinery in photoreceptors were previously demonstrated [73]. The mitochondria-related pathway may also be a common mechanism between photoreceptors and cardiomyocytes, considering the fact that both cell types include highly dense mitochondria in the cytosol. Creatinine kinase, mitochondrial 1A was also extracted as a differentially expressed gene (Table 2). Taken together, these results suggest that defects of *EYS* are involved in a common pathway between photoreceptor degeneration and dysfunction of cardiomyocytes; however, further studies are needed to confirm this hypothesis.

Although iPSC lines were established from patients with defects in *RHO* [31], *MAK* [74], *PDE6A* [75], *PRPF31* [76], *NR2E3* [77] and *EYS* [78], molecular mimicry of the iPSC-derived retina to the degenerative retina in human RP has not been confirmed. A high-throughput assay system for drug screening using human cellular models is necessary, although zebrafish model could complement such an assay [79]. The present study suggests that our cellular model may be promising for such a screening system. Our system, however, has the limitation that our photoreceptor-like cells lack other surrounding cell types, such as tissue-resident microglial cells [80] and infiltrating cells such as monocytes and lymphocytes [81], which are relevant to pathogenesis of RP. That may be why an antioxidant, NAC, did not restore decreased expression of *CRYGD* or *F2R*. However, our photoreceptor-like cells derived from EYS-RP should be a helpful cellular model, considering that rod-photoreceptor cells are primarily injured by the genetic mutations. Another limitation is that 4-PBA, which was found to restore downregulation of several EYS-associated genes, may not restore other unknown EYS-associated changes. We are planning to set up single-cell analysis to overcome this limitation. Our cellular model can be improved by using as yet undiscovered exogenous factors in the differentiation media. Furthermore, we will have to verify the present findings using other models such as iPSC-derived retinas or in vivo models in the future.

Conclusions

In summary, we here compared gene expression profiles of photoreceptor-like cells derived from dermal fibroblasts of EYS-RP patients with those of age-matched healthy donors to determine the molecular mechanism of photoreceptor degeneration in EYS-RP patients. The photoreceptor-like cells were produced by redirect differentiation with four transcription factors, CRX, RAX,

NeuroD and OTX2, as a cellular model. By global gene expression analysis, several retina-related and apoptosis/oxidative stress/ER stress/aging-related genes such as opsin gene, *CRYGD* and *F2R* were differentially expressed in EYS-RP patient-derived cells. Decreased expression levels were restored by addition of a chemical chaperone, 4-PBA. These results suggest that retinal degeneration of EYS-RP is due, at least in part, to ER stress and that the redirect differentiation method could be a valuable tool for disease model despite some limitations as a replacement for the degenerative retinas.

Abbreviations

RP: Retinitis pigmentosa; arRP: Autosomal recessive retinitis pigmentosa; EYS-RP: ArRP with defects in the *EYS* gene; 4-PBA: 4-Phenyl butyric acid; UPR: Unfolded protein response; CHOP: C/EBP homologous protein.

Supplementary Information

The online version contains supplementary material available at <https://doi.org/10.1186/s13287-022-02827-x>.

Additional file 1: Table S1. EYS-RP-associated pathways.

Additional file 2 Table S2. Primer list. **Figure S1.** Immunostaining of CRX and rhodopsin in photoreceptor-like cells derived from fibroblasts of a healthy individual (N#3) and EYS-RP (Pt#1) after 2 weeks of induction. Scale bar = 50 μ m. **Figure S2.** Comparison of the effects of pharmacological treatment on gene expression among groups, N#3 and Pt#1, with or without supplement. The same graph is shown as in Fig. 4 with other analytical results. For the sake of simplicity, comparison with the gene expression level in N#3 without any supplement (-) is shown in Fig. 4. Comparison among other groups is shown here. Column represents mean \pm SEM ($n = 6$ (N#3 without any supplement (-)), $n = 3$ (N#3 with supplement and Pt#1)). $a = p > 0.05$, $b = p > 0.01$, $c = p > 0.001$; One-way ANOVA followed by Tukey's honest test. **Figure S3.** Effect of drugs on gene expression in photoreceptor-directed fibroblasts derived from an EYS-RP patient, Pt#2. The fibroblast cells obtained from patients suffering from retinitis pigmentosa with heterozygous mutations in *EYS* gene (Pt#2) and an age-matched healthy individual (N#1) were transduced with mixture of retroviral vectors encoding CRX, RAX, NeuroD and OTX2. Gene expression was compared 2 weeks post-transduction. The differentiation media were supplemented with four drugs namely, 4-phenylbutyric acid (4-PBA; 2 mM, 5 mM and 10 mM), metformin (METF; 5 mM), rapamycin (Rapa; 4 nM, 10 nM, 20 nM, 50 nM and 100 nM), N-acetyl-L-cysteine (NAC; 10 mM) or the vehicle (EtOH) or no addition (-). The gene expression levels with different pharmacological treatments were compared to those of photoreceptor-like cells derived from a normal volunteer (N#1) without any drug or vehicle. $a = p > 0.05$, $b = p > 0.01$, $c = p > 0.001$; One-way ANOVA followed by Dunnett's test. **Figure S4.** A. Immunoblot of blue opsin and β -actin in HDF-a as negative control, photoreceptor-like cells derived from a healthy individual (N#3), EYS-RP (Pt#1) supplemented with 5 mM 4-PBA (Pt#1 + 4PBA) (panel a) and relative expression of the blue opsin (panel b). The band intensity of blue opsin was normalized by β -actin. Data represent mean \pm SEM ($n = 3$). $*p < 0.05$, $**p < 0.01$; One-way ANOVA followed by Tukey's test. B. Effect of 4-PBA in relative expression of *ERN* in EYS-RP. (a) Relative *ERN1* expression in photoreceptor-like cells derived from N#3 with/out vehicle (EtOH) and RP#1 supplemented with 5 mM 4-PBA or vehicle. (b) Relative *ERN1* expression in photoreceptor-like cells derived from Fib#1 with/out vehicle (EtOH) and RP#3 supplemented with 5 mM 4-PBA or vehicle. $*p > 0.05$; One-way ANOVA followed by Tukey's test ($n = 3$). C. a) Immunoblot of CHOP and β -actin of photoreceptor-like cells derived from fibroblasts of N#3 and RP#1 with 0 nM, 200 nM and 2 μ M thapsigargin. b) Relative expression of CHOP in photoreceptor-like cells derived from fibroblasts of N#3 and RP#1 without or without

thapsigargin with 0 nM, 200 nM and 2 μ M thapsigargin. Student's t-test ($n = 3$ (0), $n = 5$ (200 nM), $n = 5$ (2 μ M)). D. Immunoblot of cleaved caspase-3 and β -actin in HDF-a treated with 2 μ M staurosporine for 4 h before harvesting (HDF-a + Staruo) as positive control, photoreceptor-like cells derived from a healthy individual (N#3) and EYS-RP patient (Pt#1) supplemented with 5 mM 4-PBA (Pt#1 + 4PBA) (panel a) and expression level of the cleaved caspase-3 (panel b). The band intensity of cleaved caspase-3 was normalized by β -actin. Data represent mean \pm SEM ($n = 3$). * $p < 0.05$, ** $p < 0.01$; Oneway ANOVA followed by Tukey's test. **Figure S5.** Immunostaining of cleaved caspase-3 and numbers of positively stained cells in photoreceptor-directed fibroblasts of healthy individual (N#3) and EYS-RP (Pt#1) 2 weeks post-transduction supplemented by thapsigargin (1 μ M). Cells were fixed in chilled acetone at -20°C for 20 min followed by rinsing and incubated with 4% PFA in PBS for 10 min. After washing and blocking, cells were incubated with primary antibody (cleaved caspase-3 (Asp175) (5A1E) Rabbit mAb #9664, 1: 500, Cell Signaling).

Acknowledgements

We would like to express our sincere thanks to Kiyoko-Miyamoto Matsui for their technical assistance of this work. We thank the participating RP patients and healthy control subjects in this study. We sincerely appreciate staffs of the NRCD for their support for this study, especially Seishi Kato, for supervising translational research of RP in NRCD until 2020. We would like to express our sincere thanks to Catherine M. Ketcham for thoroughly reading and valuable English editing.

Author contributions

DR, YS and YK performed the experiments; YS and YT performed gene expression analysis; MI recruited patients; NA performed excision of skin tissues and for initiated us into primary culture of dermal fibroblasts; YS, DR, YK, YT and AU made experimental designs; YS, DR, YT and AU wrote the manuscript. All authors read and approved the final manuscript.

Funding

This research was supported by grants from the Japan Society for the Promotion of Science (Grant-in-Aid for Scientific Research (B) 15H04998 (to Y.S.) and 20H03845 (to Y.S.)); by Ministry of Health, Labour and Welfare Sciences (MHLW) research grants to SK (H24-kankaku-ippan-004); by the grant of National Center for Child Health and Development to AU; by grants of National Rehabilitation Center for Persons with Disabilities to YS.

Availability of data and materials

All data generated or analyzed for this study are included in this published article and the Additional file. Microarray data are deposited in the GEO with the accession number GSE199050.

Declarations

Ethics approval and consent to participate

The protocol of this study was reviewed and approved by the Ethics Committee of the NRCD. Signed informed consent was obtained from the five donors and samples were de-identified. All experiments involving human cells and tissues were performed in line with the Declaration of Helsinki.

Consent for publication

Not applicable.

Competing interests

The authors declare that they have no competing interests. Akihiro Umezawa is the Associate Editor for *Stem Cell Research & Therapy*, and he was not involved in the peer review and decision of this article.

Author details

¹Sensory Functions Section, Research Institute, National Rehabilitation Center for Persons With Disabilities, 4-1 Namiki, Tokorozawa 359-8555, Japan. ²Department of Ophthalmology, Hospital, National Rehabilitation Center for Persons With Disabilities, 4-1 Namiki, Tokorozawa 359-8555, Japan. ³Bioscience and Healthcare Engineering Division, Mitsui Knowledge Industry Co.,

Ltd., 2-7-14 Higashi-Nakano, Nakano-ku, Tokyo 164-8555, Japan. ⁴Department of Plastic, Oral and Maxillofacial Surgery, Teikyo University School of Medicine, 2-11-1 Kaga, Itabashi, Tokyo 173-8605, Japan. ⁵National Center for Child Health and Development, Research Institute, 2-10-1 Okura, Setagaya 157-8535, Japan. ⁶Present Address: Iwanami Eye Clinic, 7-1-3, Tsuchihashi, Miyamae-ku Kawasaki, Tokyo 216-0005, Japan. ⁷Present Address: Division of Bioinformation and Therapeutic Systems, National Defense Medical College, 3 Namiki, Tokorozawa 359-0042, Japan. ⁸Present Address: Miyamasuzaka Clinic, SK Aoyama Bldg. 5F, 1-6-5 Shibuya, Tokyo 150-0002, Japan.

Received: 27 December 2021 Accepted: 14 March 2022

Published online: 11 April 2022

References

1. Abd El-Aziz MM, Barragan I, O'Driscoll CA, Goodstadt L, Prigmore E, Borrego S, et al. EYS, encoding an ortholog of *Drosophila* spacemaker, is mutated in autosomal recessive retinitis pigmentosa. *Nat Genet.* 2008;40(11):1285–7.
2. Abd El-Aziz MM, O'Driscoll CA, Kaye RS, Barragan I, El-Ashry MF, Borrego S, et al. Identification of novel mutations in the ortholog of *Drosophila* eyes shut gene (EYS) causing autosomal recessive retinitis pigmentosa. *Invest Ophthalmol Vis Sci.* 2010;51(8):4266–72.
3. Bandah-Rozenfeld D, Littink KW, Ben-Yosef T, Strom TM, Chowers I, Collin RW, et al. Novel null mutations in the EYS gene are a frequent cause of autosomal recessive retinitis pigmentosa in the Israeli population. *Invest Ophthalmol Vis Sci.* 2010;51(9):4387–94.
4. Collin RW, Littink KW, Klevering BJ, van den Born LI, Koenekeop RK, Zonneveld MN, et al. Identification of a 2 Mb human ortholog of *Drosophila* eyes shut/spacemaker that is mutated in patients with retinitis pigmentosa. *Am J Hum Genet.* 2008;83(5):594–603.
5. Iwanami M, Oshikawa M, Nishida T, Nakadomari S, Kato S. High prevalence of mutations in the EYS gene in Japanese patients with autosomal recessive retinitis pigmentosa. *Invest Ophthalmol Vis Sci.* 2012;53(2):1033–40.
6. Hosono K, Ishigami C, Takahashi M, Park DH, Hiram Y, Nakanishi H, et al. Two novel mutations in the EYS gene are possible major causes of autosomal recessive retinitis pigmentosa in the Japanese population. *PLoS ONE.* 2012;7(2):e31036.
7. Iwanami M, Oishi A, Ogino K, Seko Y, Nishida-Shimizu T, Yoshimura N, et al. Five major sequence variants and copy number variants in the EYS gene account for one-third of Japanese patients with autosomal recessive and simplex retinitis pigmentosa. *Mol Vis.* 2019;25:766–79.
8. Koyanagi Y, Akiyama M, Nishiguchi KM, Momozawa Y, Kamatani Y, Takata S, et al. Genetic characteristics of retinitis pigmentosa in 1204 Japanese patients. *J Med Genet.* 2019;56(10):662–70.
9. Yang L, Fujinami K, Ueno S, Kuniyoshi K, Hayashi T, Kondo M, et al. Genetic spectrum of EYS-associated retinal disease in a Large Japanese Cohort: identification of disease-associated variants with relatively high allele frequency. *Sci Rep.* 2020;10(1):5497.
10. Bainbridge JW, Smith AJ, Barker SS, Robbie S, Henderson R, Balaggan K, et al. Effect of gene therapy on visual function in Leber's congenital amaurosis. *N Engl J Med.* 2008;358(21):2231–9.
11. Maguire AM, Simonelli F, Pierce EA, Pugh EN Jr, Mingozzi F, Bennicelli J, et al. Safety and efficacy of gene transfer for Leber's congenital amaurosis. *N Engl J Med.* 2008;358(21):2240–8.
12. Fry LE, McClements ME, MacLaren RE. Analysis of pathogenic variants correctable with CRISPR base editing among patients with recessive inherited retinal degeneration. *JAMA Ophthalmol.* 2021;139(3):319–28.
13. Nishiguchi KM, Miya F, Mori Y, Fujita K, Akiyama M, Kamatani T, et al. A hypomorphic variant in EYS detected by genome-wide association study contributes toward retinitis pigmentosa. *Commun Biol.* 2021;4(1):140.
14. Duricka DL, Brown RL, Varnum MD. Defective trafficking of cone photoreceptor CNG channels induces the unfolded protein response and ER-stress-associated cell death. *Biochem J.* 2012;441(2):685–96.
15. Yoshida N, Ikeda Y, Notomi S, Ishikawa K, Murakami Y, Hisatomi T, et al. Laboratory evidence of sustained chronic inflammatory reaction in retinitis pigmentosa. *Ophthalmology.* 2013;120(1):e5–12.

16. Ikeda HO, Sasaoka N, Koike M, Nakano N, Muraoka Y, Toda Y, et al. Novel VCP modulators mitigate major pathologies of rd10, a mouse model of retinitis pigmentosa. *Sci Rep*. 2014;4:5970.
17. Luodan A, Zou T, He J, Chen X, Sun D, Fan X, et al. Rescue of retinal degeneration in rd1 mice by intravitreally injected metformin. *Front Mol Neurosci*. 2019;12:102.
18. Jin ZB, Okamoto S, Osakada F, Homma K, Assawachananont J, Hirami Y, et al. Modelling retinal degeneration using patient-specific induced pluripotent stem cells. *PLoS ONE*. 2011;6(2):e17084.
19. Jin ZB, Okamoto S, Xiang P, Takahashi M. Integration-free induced pluripotent stem cells derived from retinitis pigmentosa patient for disease modeling. *Stem Cells Transl Med*. 2012;1(6):503–9.
20. Ohlemacher SK, Iglesias CL, Sridhar A, Gamm DM, Meyer JS. Generation of highly enriched populations of optic vesicle-like retinal cells from human pluripotent stem cells. *Curr Protoc Stem Cell Biol*. 2015;32:1H 8 1-H 8 20.
21. Osakada F, Jin ZB, Hirami Y, Ikeda H, Danjyo T, Watanabe K, et al. In vitro differentiation of retinal cells from human pluripotent stem cells by small-molecule induction. *J Cell Sci*. 2009;122(Pt 17):3169–79.
22. Akagi T, Akita J, Haruta M, Suzuki T, Honda Y, Inoue T, et al. Iris-derived cells from adult rodents and primates adopt photoreceptor-specific phenotypes. *Invest Ophthalmol Vis Sci*. 2005;46(9):3411–9.
23. Seko Y, Azuma N, Kaneda M, Nakatani K, Miyagawa Y, Noshiro Y, et al. Derivation of human differential photoreceptor-like cells from the iris by defined combinations of CRX, RX and NEUROD. *PLoS ONE*. 2012;7(4):e35611.
24. Seko Y, Azuma N, Ishii T, Komuta Y, Miyamoto K, Miyagawa Y, et al. Derivation of human differential photoreceptor cells from adult human dermal fibroblasts by defined combinations of CRX, RAX, OTX2 and NEUROD. *Genes Cells*. 2014;19(3):198–208.
25. Komuta Y, Ishii T, Kaneda M, Ueda Y, Miyamoto K, Toyoda M, et al. In vitro transdifferentiation of human peripheral blood mononuclear cells to photoreceptor-like cells. *Biol Open*. 2016;5(6):709–19.
26. Seko Y, Iwanami M, Miyamoto-Matsui K, Takita S, Aoi N, Umezawa A, et al. The manner of decay of genetically defective EYS gene transcripts in photoreceptor-directed fibroblasts derived from retinitis pigmentosa patients depends on the type of mutation. *Stem Cell Res Ther*. 2018;9(1):279.
27. Lu Z, Hu X, Liu F, Soares DC, Liu X, Yu S, et al. Ablation of EYS in zebrafish causes mislocalisation of outer segment proteins, F-actin disruption and cone-rod dystrophy. *Sci Rep*. 2017;7:46098.
28. Wullschlegel S, Loewith R, Hall MN. TOR signaling in growth and metabolism. *Cell*. 2006;124(3):471–84.
29. Zhang L, Justus S, Xu Y, Pluchenik T, Hsu CW, Yang J, et al. Reprogramming towards anabolism impedes degeneration in a preclinical model of retinitis pigmentosa. *Hum Mol Genet*. 2016;25(19):4244–55.
30. Yang JL, Zou TD, Yang F, Yang ZL, Zhang HB. Inhibition of mTOR signaling by rapamycin protects photoreceptors from degeneration in rd1 mice. *Zool Res*. 2021;42(4):482–6.
31. Yoshida T, Ozawa Y, Suzuki K, Yuki K, Ohyama M, Akamatsu W, et al. The use of induced pluripotent stem cells to reveal pathogenic gene mutations and explore treatments for retinitis pigmentosa. *Mol Brain*. 2014;7:45.
32. Choi SI, Lee E, Jeong JB, Akuzum B, Maeng YS, Kim TI, et al. 4-Phenylbutyric acid reduces mutant-TGFBp levels and ER stress through activation of ERAD pathway in corneal fibroblasts of granular corneal dystrophy type 2. *Biochem Biophys Res Commun*. 2016;477(4):841–6.
33. Yu M, Liu Y, Li J, Natale BN, Cao S, Wang D, et al. Eyes shut homolog is required for maintaining the ciliary pocket and survival of photoreceptors in zebrafish. *Biol Open*. 2016;5(11):1662–73.
34. Cottet S, Schorderet DF. Mechanisms of apoptosis in retinitis pigmentosa. *Curr Mol Med*. 2009;9(3):375–83.
35. Piano I, D'Antongiovanni V, Testai L, Calderone V, Gargini C. A nutraceutical strategy to slowing down the progression of cone death in an animal model of retinitis pigmentosa. *Front Neurosci*. 2019;13:461.
36. Athanasiou D, Aguila M, Bellingham J, Kanuga N, Adamson P, Cheetham ME. The role of the ER stress-response protein PERK in rhodopsin retinitis pigmentosa. *Hum Mol Genet*. 2017;26(24):4896–905.
37. Athanasiou D, Aguila M, Bellingham J, Li W, McCulley C, Reeves PJ, et al. The molecular and cellular basis of rhodopsin retinitis pigmentosa reveals potential strategies for therapy. *Prog Retin Eye Res*. 2018;62:1–23.
38. Hollien J, Weissman JS. Decay of endoplasmic reticulum-localized mRNAs during the unfolded protein response. *Science*. 2006;313(5783):104–7.
39. Adams CJ, Kopp MC, Larburu N, Nowak PR, Ali MMU. Structure and molecular mechanism of ER stress signaling by the unfolded protein response signal activator IRE1. *Front Mol Biosci*. 2019;6:11.
40. Junjappa RP, Patil P, Bhattarai KR, Kim HR, Chae HJ. IRE1a Implications in endoplasmic reticulum stress-mediated development and pathogenesis of autoimmune diseases. *Front Immunol*. 2018;9:1289.
41. Roshan M, Vijaya PH, Lavanya GR, Shama PK, Santhiya ST, Graw J, et al. A novel human CRYGD mutation in a juvenile autosomal dominant cataract. *Mol Vis*. 2010;16:887–96.
42. Knopfel EB, Vilches C, Camargo SMR, Errasti-Murugarren E, Staubli A, Mayayo C, et al. Dysfunctional LAT2 amino acid transporter is associated with cataract in mouse and humans. *Front Physiol*. 2019;10:688.
43. Sun Y, Li JK, He W, Wang ZS, Bai JY, Xu L, et al. Genetic and clinical analysis in Chinese patients with retinitis pigmentosa caused by EYS mutations. *Mol Genet Genomic Med*. 2020;8(3):e1117.
44. Sun Y, Li W, Li JK, Wang ZS, Bai JY, Xu L, et al. Genetic and clinical findings of panel-based targeted exome sequencing in a northeast Chinese cohort with retinitis pigmentosa. *Mol Genet Genomic Med*. 2020;8(4):e1184.
45. Hong Y, Li H, Sun Y, Ji Y. A review of complicated cataract in retinitis pigmentosa: pathogenesis and cataract surgery. *J Ophthalmol*. 2020;2020:6699103.
46. Barabino A, Flamier A, Hanna R, Heon E, Freedman BS, Bernier G. Deregulation of neuro-developmental genes and primary cilium cytoskeleton anomalies in iPSC retinal sheets from human syndromic ciliopathies. *Stem Cell Rep*. 2020;14(3):357–73.
47. Abu-Hussien M, Viswanathan GK, Haj E, Paul A, Gazit E, Segal D. An amyloidogenic hexapeptide from the cataract-associated gammaD-crystallin is a model for the full-length protein and is inhibited by naphthoquinone-tryptophan hybrids. *Int J Biol Macromol*. 2020;157:424–33.
48. Haarman AEG, Enthoven CA, Tedja MS, Polling JR, Tideman JWL, Keunen JEE, et al. Phenotypic consequences of the GJD2 risk genotype in myopia development. *Invest Ophthalmol Vis Sci*. 2021;62(10):16.
49. Kantor O, Benko Z, Enzsoly A, David C, Naumann A, Nitschke R, et al. Characterization of connexin36 gap junctions in the human outer retina. *Brain Struct Funct*. 2016;221(6):2963–84.
50. Deans MR, Volgyi B, Goodenough DA, Bloomfield SA, Paul DL. Connexin36 is essential for transmission of rod-mediated visual signals in the mammalian retina. *Neuron*. 2002;36(4):703–12.
51. Husain N, Pellikka M, Hong H, Klimentova T, Choe KM, Clandinin TR, et al. The agrin/perlecan-related protein eyes shut is essential for epithelial lumen formation in the Drosophila retina. *Dev Cell*. 2006;11(4):483–93.
52. Liu Y, Yu M, Shang X, Nguyen MHH, Balakrishnan S, Sager R, et al. Eyes shut homolog (EYS) interacts with matriglycan of O-mannosyl glycans whose deficiency results in EYS mislocalization and degeneration of photoreceptors. *Sci Rep*. 2020;10(1):7795.
53. Messchaert M, Dona M, Broekman S, Peters TA, Corral-Serrano JC, Slijkerman RWN, et al. Eyes shut homolog is important for the maintenance of photoreceptor morphology and visual function in zebrafish. *PLoS ONE*. 2018;13(7):e0200789.
54. Rehemtulla A, Warwar R, Kumar R, Ji X, Zack DJ, Swaroop A. The basic motif-leucine zipper transcription factor Nr1 can positively regulate rhodopsin gene expression. *Proc Natl Acad Sci USA*. 1996;93(1):191–5.
55. Mears AJ, Kondo M, Swain PK, Takada Y, Bush RA, Saunders TL, et al. Nr1 is required for rod photoreceptor development. *Nat Genet*. 2001;29(4):447–52.
56. Banin E, Cideciyan AV, Aleman TS, Petters RM, Wong F, Milam AH, et al. Retinal rod photoreceptor-specific gene mutation perturbs cone pathway development. *Neuron*. 1999;23(3):549–57.
57. Littink KW, van den Born LI, Koenekoop RK, Collin RW, Zonneveld MN, Blokland EA, et al. Mutations in the EYS gene account for approximately 5% of autosomal recessive retinitis pigmentosa and cause a fairly homogeneous phenotype. *Ophthalmology*. 2010;117(10):2026–33, 33 e1–7.
58. Pierrache LHM, Messchaert M, Thiadens A, Haer-Wigman L, de Jong-Hesse Y, van Zelst-Stams WAG, et al. Extending the spectrum of EYS-associated retinal disease to macular dystrophy. *Invest Ophthalmol Vis Sci*. 2019;60(6):2049–63.

59. Georgiou M, Grewal PS, Narayan A, Alser M, Ali N, Fujinami K, et al. Sector retinitis pigmentosa: extending the molecular genetics basis and elucidating the natural history. *Am J Ophthalmol*. 2021;221:299–310.
60. Marques JP, Porto FBO, Carvalho AL, Neves E, Chen R, Sampaio SAM, et al. EYS-associated sector retinitis pigmentosa. *Graefes Arch Clin Exp Ophthalmol*. 2021;260:1405–13.
61. Komeima K, Rogers BS, Lu L, Campochiaro PA. Antioxidants reduce cone cell death in a model of retinitis pigmentosa. *Proc Natl Acad Sci USA*. 2006;103(30):11300–5.
62. Punzo C, Kornacker K, Cepko CL. Stimulation of the insulin/mTOR pathway delays cone death in a mouse model of retinitis pigmentosa. *Nat Neurosci*. 2009;12(1):44–52.
63. Silverman SM, Ma W, Wang X, Zhao L, Wong WT. C3- and CR3-dependent microglial clearance protects photoreceptors in retinitis pigmentosa. *J Exp Med*. 2019;216(8):1925–43.
64. Okita A, Murakami Y, Shimokawa S, Funatsu J, Fujiwara K, Nakatake S, et al. Changes of serum inflammatory molecules and their relationships with visual function in retinitis pigmentosa. *Invest Ophthalmol Vis Sci*. 2020;61(11):30.
65. Guo H, Liu D, Gelbard H, Cheng T, Insalaco R, Fernandez JA, et al. Activated protein C prevents neuronal apoptosis via protease activated receptors 1 and 3. *Neuron*. 2004;41(4):563–72.
66. Pichaud F. PAR-complex and crumbs function during photoreceptor morphogenesis and retinal degeneration. *Front Cell Neurosci*. 2018;12:90.
67. Tantivejkul K, Loberg RD, Mawocha SC, Day LL, John LS, Pienta BA, et al. PAR1-mediated NFκB activation promotes survival of prostate cancer cells through a Bcl-xL-dependent mechanism. *J Cell Biochem*. 2005;96(3):641–52.
68. Hetz C, Zhang K, Kaufman RJ. Mechanisms, regulation and functions of the unfolded protein response. *Nat Rev Mol Cell Biol*. 2020;21(8):421–38.
69. Lobo GP, Ebke LA, Au A, Hagstrom SA. TULP1 missense mutations induces the endoplasmic reticulum unfolded protein response stress complex (ER-UPR). *Adv Exp Med Biol*. 2016;854:223–30.
70. Coelho DS, Cairrão F, Zeng X, Pires E, Coelho AV, Ron D, et al. Xbp1-independent Ire1 signaling is required for photoreceptor differentiation and rhodopsin morphogenesis in *Drosophila*. *Cell Rep*. 2013;5(3):791–801.
71. Garcia-Delgado AB, Valdes-Sanchez L, Morillo-Sanchez MJ, Ponte-Zuniga B, Diaz-Corrales FJ, de la Cerda B. Dissecting the role of EYS in retinal degeneration: clinical and molecular aspects and its implications for future therapy. *Orphanet J Rare Dis*. 2021;16(1):222.
72. Udagawa C, Nakamura H, Ohnishi H, Tamura K, Shimoi T, Yoshida M, et al. Whole exome sequencing to identify genetic markers for trastuzumab-induced cardiotoxicity. *Cancer Sci*. 2018;109(2):446–52.
73. Nie J, Mahato S, Zelhof AC. The actomyosin machinery is required for *Drosophila* retinal lumen formation. *PLoS Genet*. 2014;10(9):e1004608.
74. Tucker BA, Scheetz TE, Mullins RF, DeLuca AP, Hoffmann JM, Johnston RM, et al. Exome sequencing and analysis of induced pluripotent stem cells identify the cilia-related gene male germ cell-associated kinase (MAK) as a cause of retinitis pigmentosa. *Proc Natl Acad Sci USA*. 2011;108(34):E569–76.
75. Riera M, Patel A, Corcostegui B, Chang S, Sparrow JR, Pomares E, et al. Establishment and characterization of an iPSC line (FRIMO1001-A) derived from a retinitis pigmentosa patient carrying PDE6A mutations. *Stem Cell Res*. 2019;35:101385.
76. McLenachan S, Zhang D, Zhang X, Chen SC, Lamey T, Thompson JA, et al. Generation of two induced pluripotent stem cell lines from a patient with dominant PRPF31 mutation and a related non-penetrant carrier. *Stem Cell Res*. 2019;34:101357.
77. Terray A, Slembrouck A, Nanteau C, Chondroyer C, Zeitz C, Sahel JA, et al. Generation of an induced pluripotent stem cell (iPSC) line from a patient with autosomal dominant retinitis pigmentosa due to a mutation in the NR2E3 gene. *Stem Cell Res*. 2017;24:1–4.
78. Calado SM, Garcia-Delgado AB, De la Cerda B, Ponte-Zuniga B, Bhat-tacharya SS, Diaz-Corrales FJ. Generation of a human iPSC cell line from a patient with retinitis pigmentosa due to EYS mutation. *Stem Cell Res*. 2018;33:251–4.
79. Alhasani RH, Zhou X, Biswas L, Li X, Reilly J, Zeng Z, et al. Gypenosides attenuate retinal degeneration in a zebrafish retinitis pigmentosa model. *Exp Eye Res*. 2020;201:108291.
80. Karlstetter M, Scholz R, Rutar M, Wong WT, Provis JM, Langmann T. Retinal microglia: just bystander or target for therapy? *Prog Retin Eye Res*. 2015;45:30–57.
81. Saban DR. New concepts in macrophage ontogeny in the adult neural retina. *Cell Immunol*. 2018;330:79–85.

Publisher's Note

Springer Nature remains neutral with regard to jurisdictional claims in published maps and institutional affiliations.

Ready to submit your research? Choose BMC and benefit from:

- fast, convenient online submission
- thorough peer review by experienced researchers in your field
- rapid publication on acceptance
- support for research data, including large and complex data types
- gold Open Access which fosters wider collaboration and increased citations
- maximum visibility for your research: over 100M website views per year

At BMC, research is always in progress.

Learn more biomedcentral.com/submissions

